Green Synthesis of TiO_2 Using Sappan Wood (*Biancaea sappan* L.) Extract as a Bioreductant and Evaluation of Its Antibacterial Activity

Risya Sasri*, Vika Vika, Adhitiyawarman Adhitiyawarman, and Winda Rahmalia

Department of Chemistry, Faculty of Mathematics and Natural Sciences, Universitas Tanjungpura, Jl. Prof. Dr. H. Hadari Nawawi, Pontianak 78124, Indonesia

* **Corresponding author:**

email: risya@untan.ac.id

Received: January 15, 2026
Accepted: May 27, 2026

DOI: 10.22146/ijc.115655

Abstract: *This study aimed to synthesize TiO_2 via green synthesis using* Biancaea sappan *L. (sappan wood) extract as a reducing and stabilizing agent, as well as to evaluate their antibacterial activity against* Escherichia coli *and* Staphylococcus aureus*. The TiO_2 was synthesized using two methods: green synthesis and conventional synthesis. Titanium(IV) tetraisopropoxide was used as the precursor and the volume of the extract was varied (14, 25, and 33% (v/v)) relative to the total volume to assess their influence on the characteristics of the TiO_2. FTIR characterization indicated that bioactive compounds from sappan wood extract, particularly brazilin, played a significant role as reducing agents. XRD and UV-vis DRS analyses showed that the TiO_2 had an anatase crystalline phase with an average crystallite size of 15.84–19.75 nm and a band gap of 2.53–3.03 eV. Antibacterial activity was assessed using the disc diffusion method under visible light and UV irradiation to evaluate the inhibition of* E. coli *and* S. aureus *bacteria. The results demonstrated that green-synthesized TiO_2 exhibited antibacterial activity against both* E. coli *and* S. aureus *under UV irradiation. This research presents new opportunities for green-synthesized TiO_2 as environmentally friendly and sustainable antibacterial agents.*

Keywords: *green synthesis; titanium dioxide (TiO_2);* Biancaea sappan *L.;* Escherichia coli; Staphylococcus aureus

INTRODUCTION

Titanium dioxide (TiO_2), also known as titania, is a metal oxide widely utilized in photocatalytic applications [1]. The properties of TiO_2, such as high chemical stability, high refractive index, and the presence of oxygen-containing functional groups within its crystal lattice, make it a widely used material as a semiconductor. Several synthesis methods, including chemical vapor deposition, electrochemical deposition, the sol-gel technique, hydrothermal crystallization, and chemical precipitation, are commonly employed in TiO_2 synthesis. However, these methods often involve hazardous chemicals, such as acetylacetonate as a stabilizing agent, as well as high-energy processes, both of which pose negative impacts on the environment, potential risks to human health, and high energy consumption. An alternative approach to minimize such impacts is the application of green synthesis methods [2].

Green synthesis is a method for synthesizing metal particles using environmentally friendly procedures and natural materials [2]. In green synthesis, natural substances serve as stabilizing agents, thereby reducing the use of harmful chemical agents. Metal particle synthesis via green synthesis can be carried out using bacteria, actinomycetes, algae, fungi, yeast, or plant extracts. Among these, the use of plant extracts is considered a simpler and more feasible approach for large-scale production of metal particles compared to synthesis mediated by bacteria and fungi [3].

Plant extracts contain phytochemical compounds such as flavonoids, phenolic acids, and terpenoids, which possess functional groups (e.g., hydroxyl and carbonyl groups) capable of coordinating with Ti^{4+} ions. This interaction allows phytochemical compounds to act as capping and stabilizing agents by adsorbing onto the surface of TiO_2 nanoparticles and preventing aggregation. This stabilization mechanism is functionally comparable to acetylacetonate, which stabilizes metal precursors through coordination interactions. Research conducted by Insuan [4] revealed that sappan wood (*Biancaea sappan* L.) extract contains flavonoids. These active compounds play a role in the synthesis of TiO_2. Moreover, the bioactive compounds in sappan wood extract also exhibit antibacterial and antioxidant activities [3].

In addition to its excellent photocatalytic activity, TiO_2 is also known for its antibacterial properties. Research by Younis el al. [5] demonstrated that TiO_2 exhibits antibacterial activity against *Escherichia coli* and *Staphylococcus aureus*. The high oxidative properties of TiO_2 enable it to generate free radicals capable of damaging bacterial cell walls, thereby inhibiting the growth and proliferation of pathogenic microorganisms. Based on cell wall structure, bacteria are classified into two groups; Gram-positive and Gram-negative. The differences in cell wall structure influence the antibacterial activity of TiO_2. Gram-positive bacteria possess a thick peptidoglycan layer, whereas Gram-negative bacteria have an outer lipopolysaccharide membrane [6].

Based on the above considerations, this study was conducted to investigate the characteristics and antibacterial activity of TiO_2 synthesized using *B. sappan* L. extract. The antibacterial activity of TiO_2 was evaluated against *E. coli* as a Gram-negative bacterium and *S. aureus* as a Gram-positive bacterium. Furthermore, X-ray diffraction (XRD) analysis was performed to determine the crystalline phase and size, diffuse reflectance spectroscopy (UV-vis DRS) to determine the band gap energy of the obtained TiO_2, and Fourier transform infrared spectrometry (FTIR) to identify functional groups and interactions formed in the TiO_2 synthesized using *B. sappan* L. extract.

■ EXPERIMENTAL SECTION

Materials

The materials used in this study included distilled water, acetic acid (CH_3COOH), hydrochloric acid (HCl) 37%, sulfuric acid (H_2SO_4, Merck), iron(III) chloride ($FeCl_3$) 1%, dimethyl sulfoxide (DMSO, Merck), ethanol (Merck), commercial sappan wood (*B. sappan* L.), magnesium (Mg), nutrient agar (NA, Himedia), streptomycin sulfate (Meiji), and titanium(IV) tetraisopropoxide 97% ($Ti(OCH(CH_3)_2)_4$, Sigma-Aldrich).

Instrumentation

Analytical instruments used included a FTIR spectrophotometer (Shimadzu IR Prestige-21), an XRD instrument (Bruker D2-Phaser), and a UV-vis DRS spectrophotometer (Perkin Elmer 365+).

Procedure

Sappan wood extraction

The procedure in this experiment was adapted from the study by Kaur [3], with modifications in the amount of sample used. Sappan wood chips were cut into smaller pieces using scissors. A total of 10 g of sappan wood chips was weighed and mixed with 100 mL of ethanol. The mixture was extracted at 50 °C for 1 h. The resulting mixture was then filtered, and the filtrate was collected. The filtrate, in the form of sappan wood ethanol extract, was stored in a closed container protected from light.

Phytochemical test of sappan wood extract

Phytochemical screening of sappan wood extract was carried out to examine the active compound components, including alkaloids, phenolics, flavonoids, saponins, steroids, and terpenoids. The experimental procedure followed the method of Dubale et al. [7], with modifications to the tested samples. Phytochemical screening of active compounds was conducted as follows:

Alkaloid identification. Concentrated sappan wood extract was placed into three different test tubes, each containing 20 drops. Test tube 1 was added with 2 drops of Mayer's reagent, test tube 2 with 2 drops of Wagner's reagent, and test tube 3 with 2 drops of Dragendorff's reagent. Each tube was shaken and the resulting changes were observed.

Phenolic identification. A total of 20 drops of concentrated sappan wood extract was placed in a test tube. Two drops of 1% $FeCl_3$ solution were added, then shaken, and the resulting changes were observed.

Flavonoid identification. Twenty drops of concentrated sappan wood extract obtained from evaporation were placed in a test tube. Mg powder (0.1 g) and 2 drops of concentrated HCl were added, then shaken, and the resulting changes were observed.

Saponin Identification. Twenty drops of concentrated sappan wood extract were placed in a test tube. The sample was vigorously shaken and left to stand for 5 min.

Steroid and terpenoid identification. Twenty drops of concentrated sappan wood extract were placed in a test tube. Two drops of acetic anhydride and concentrated H_2SO_4 were added, then shaken, and the resulting changes were observed.

Green synthesis of TiO_2

The experimental procedure was adapted from the study by Mathew et al. [8] with modifications using sappan wood extract as a natural bioreductor in the process. The synthesis was carried out with variations of extract volume: 5 mL (TiO_2-14%), 10 mL (TiO_2-25%), and 15 mL (TiO_2-33%), with percentages based on the ratio of extract volume to solvent and precursor. The TiO_2 synthesis was initiated by adding 25 mL of absolute ethanol to a beaker, followed by 5 mL of TTIP. The extract was then added according to the variation. The mixture was heated at 50 °C and stirred for 2 h. The resulting product was filtered, and the residue was dried at 80 °C for 16 h. The dried residue was ground and subsequently calcined at 500 °C for 2 h. The obtained TiO_2 particles were reground and stored in a tightly sealed container for further characterization using FTIR, XRD, and UV-vis DRS. The results of the subsequent synthesis are denoted TiO_2-14%, TiO_2-25%, and TiO_2-33%.

Conventional synthesis of TiO_2

The experimental procedure was adapted from the study conducted by De Luca et al. [9]. Conventional TiO_2 synthesis was carried out by mixing 20 mL of water and 5 mL of ethanol. A total of 5 mL of TTIP was added to the water-ethanol mixture and stirred for 1 h. HNO_3 was then added until the solution reached pH 2, followed by further stirring for 1 h. The mixture was filtered to obtain the residue, which was dried at 80 °C for 16 h and subsequently calcined at 500 °C for 2 h. The resulting TiO_2 particles were ground and stored in a tightly sealed container for further characterization using FTIR, XRD, and UV-vis DRS. The results of the subsequent synthesis are denoted TiO_2-C as the control sample, synthesized using the conventional method without the addition of sappan wood extract.

Antibacterial activity test of TiO_2

The test procedure was adapted from the study conducted by Subhapriya [10], with modifications in the test samples used. First, TiO_2 suspensions were prepared by weighing 30.0 mg each of TiO_2-C, TiO_2-14%, TiO_2-25%, and TiO_2-33%. An amount of 1 mL of 1% DMSO was added to each Erlenmeyer flask containing the sample, followed by sonication for 30 min to obtain the TiO_2 suspensions. The procedure continued by streaking overnight-incubated bacterial cultures of *E. coli* and *S. aureus* onto NA plates using a cotton swab. Sterile paper discs (6 mm diameter) were placed on the agar surface, and 15 µL of the test samples, including sappan wood extract, TiO_2-C, TiO_2-14%, TiO_2-25%, and TiO_2-33% suspensions (450 µg/mL) were dropped onto each disc. DMSO served as the negative control, while streptomycin was used as the positive control. The culture media were incubated at room temperature for 24 h under both visible light and UV irradiation. After incubation, the inhibition zones formed were measured using a vernier caliper.

■ RESULTS AND DISCUSSION

Ethanol extract of sappan wood was used as a natural reducing and stabilizing agent in the green synthesis of TiO_2 nanoparticles. The resulting extract was rich in phytochemicals and was used for phytochemical analysis and nanoparticle synthesis. Before synthesis, the extract was subjected to phytochemical screening to identify the bioactive constituents potentially involved in nanoparticle formation and surface modification. The use of sappan wood extract is particularly attractive in green chemistry approaches due to its rich phenolic and flavonoid content, which may contribute to the reduction process and influence the physicochemical properties of the resulting TiO_2 nanomaterials.

Phytochemical analysis was conducted to identify the bioactive compounds present in the sappan wood extract. The phytochemical tests in this study targeted alkaloids, phenolics, flavonoids, saponins, steroids, and terpenoids. A positive result for each class of bioactive compounds was indicated by a color change or the formation of a precipitate after the addition of specific reagents. The observed changes are presented in Fig. 1. The results summarized in Table 1 indicate that the sappan wood extract tested positive for phenolics, flavonoids, and terpenoids.

Alkaloid content was tested using Mayer's, Wagner's, and Dragendorff's reagents. A positive result with Mayer's reagent is indicated by the formation of a white precipitate, with Wagner's reagent by a brown precipitate, and with Dragendorff's reagent by an orange precipitate [11]. In this study, the solution remained red and no precipitate was formed, indicating that the sappan wood extract tested negative for alkaloids. Phenolic content was examined using a 1% $FeCl_3$ solution. A positive result is indicated by the formation of a green, blue, or black solution [12]. In this study, the test yielded a positive result for phenolics, as the solution turned black. The phenolic compounds present in sappan wood, such as chlorogenic acid, caffeic acid, and gallic acid, are likely to play a key role as stabilizing agents. These compounds contain hydroxyl and carbonyl functional groups that can coordinate with Ti^{4+} ions and adsorb onto the surface of TiO_2 particles, thereby acting as capping agents that inhibit aggregation and improve particle stability [13].

Flavonoid content in this study was tested using Mg powder and concentrated HCl. A positive result is indicated by the formation of a red solution [11]. Based on the test results, the extract showed a positive reaction for flavonoids, as the solution turned deep red. The flavonoid compounds present in sappan wood, such as brazilin, hematoxylin, and protosappanin, are likely to contribute to the stabilization of TiO_2 nanoparticles. These compounds contain multiple hydroxyl groups that can coordinate with Ti^{4+} ions and adsorb onto the particle surface, thereby acting as capping agents that inhibit aggregation and improve stability [13]. Saponin content was tested by vigorously shaking the sample and observing the foam formation. The presence of stable foam indicates a positive result for saponins [12]. In this study, a negative result was obtained, as the foam formed was minimal and unstable.

Steroid and terpenoid contents were tested using the same reagents, namely acetic anhydride and concentrated H_2SO_4. A positive result for steroids is indicated by the formation of a blue or green solution, whereas the formation of a reddish-brown solution indicates the presence of terpenoids [12]. In this study, a positive result for terpenoids was obtained, as indicated by the formation of a red solution. The terpenoid compounds present in sappan wood, such as lupeol, β-amyrin, and cycloartenol, may contribute to nanoparticle stabilization by acting as surface-active agents. These compounds can adsorb onto the surface of

Table 1. Phytochemical test result of sappan wood extract

Secondary metabolite compounds	Sappan wood extract	
	Observation	Result
Alkaloids	No changes occurred	-
Phenolics	Black solution	+
Flavonoids	Concentrated red solution	+
Saponins	Unsable foam	-
Steroids	No changes occurred	-
Terpenoids	Red Solution	+

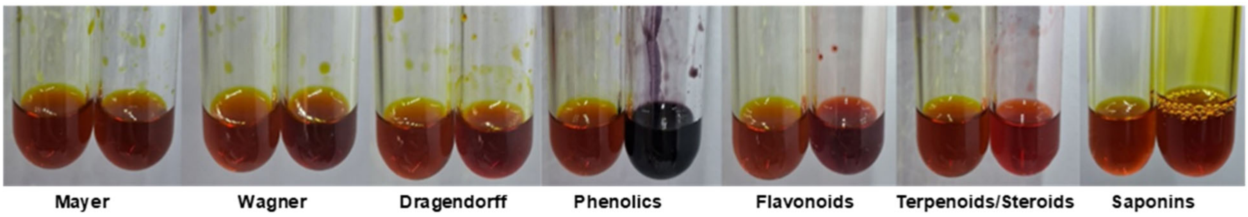

Fig 1. Phytochemical test result of sappan wood extract

TiO_2 particles, forming a protective layer that reduces segregation. Their role complements that of phenolic and flavonoid compounds, which primarily stabilize particles through coordination interactions [13].

In this study, TiO_2 was synthesized using two methods: green synthesis and the conventional method. Green synthesis predominantly utilizes plants rather than bacteria, fungi, algae, and others as capping agents, reducing agents, and stabilizers. This is due to the presence of various phytochemicals in plants, such as alkaloids, phenols, tannins, terpenoids, steroids alkaloids, phenols, tannins, terpenoids, steroids, as well as other phytochemicals such as saponins, glycosides, and proteins which may also contribute to reduction, capping, and stabilization processes. In addition, plants are readily available and require fewer steps in the synthesis of metal particles [14]. According to Aslam et al. [15], green synthesis of TiO_2 with the aid of bioactive compounds generally consists of three stages. The first stage is activation, in which metal ions are reduced and nucleation occurs. The second stage is growth, where particle nucleic merge to form larger particles as their thermodynamic stability increases. The final stage determines the morphology of the metal particles through termination reactions.

The mechanism of TiO_2 formation involves the hydrolysis of a titanium precursor (TTIP) to form Ti–OH species, followed by condensation to form a Ti–O–Ti network, leading to the nucleation and growth of TiO_2 nanoparticles. Phytochemical compounds present in the extract interact with this process. Among the phytochemical compounds, phenolic compounds and flavonoids (such as brazilin, hematoxylin, protosappanin, and phenolic acids) are thought to play a more dominant role as stabilizing and capping agents due to the presence of several hydroxyl and carbonyl functional groups that can coordinate with Ti^{4+} ions and adsorb onto the nanoparticle surface. This interaction helps control nucleation and prevent aggregation. Terpenoid compounds may also contribute, but primarily as surface-active agents with a secondary role in stabilization. An illustration of the green synthesis of TiO_2 using sappan wood extract is shown in Fig. 2.

The green synthesis method in this study was a modification of the procedure previously reported by Mathew et al. [8]. In this synthesis, sappan extract was employed as a natural bioreducing agent. The process was carried out by varying the extract volumes (5, 10, and 15 mL) to evaluate their effect on the characteristics of the synthesized TiO_2. The obtained TiO_2 is shown in Fig. 3, appearing as a grayish powder and labeled according to the extract volume used: 5 mL (TiO_2-14%), 10 mL (TiO_2-25%), and 15 mL (TiO_2-33%). The yields of the synthesized TiO_2 were 18.95, 26.45, and 27.91%, respectively.

The conventional synthesis of TiO_2 in this study was adapted from the method reported by De Luca et al. [9]. The experiment was carried out by adding TTIP

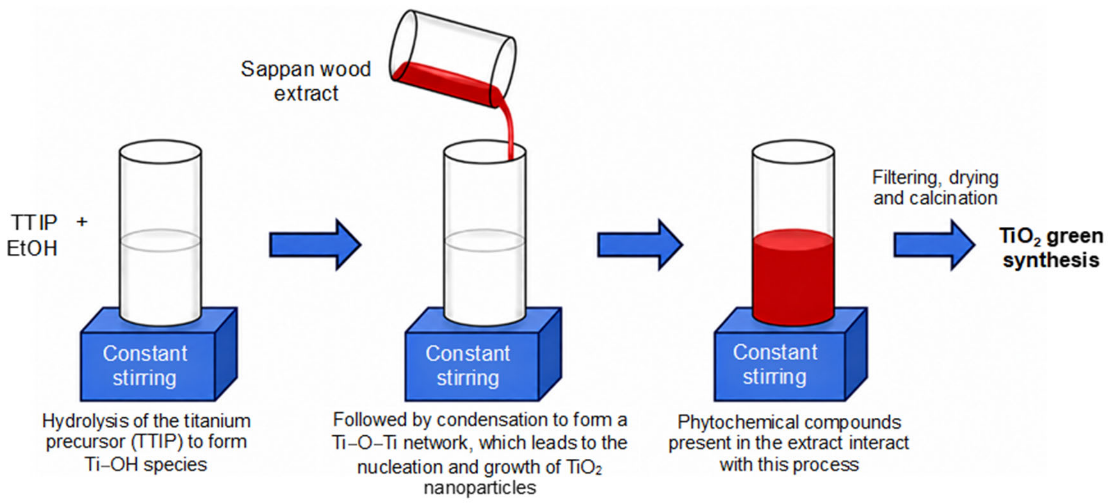

Fig 2. Schematic illustration of TiO_2 formation via green synthesis using sappan wood extract

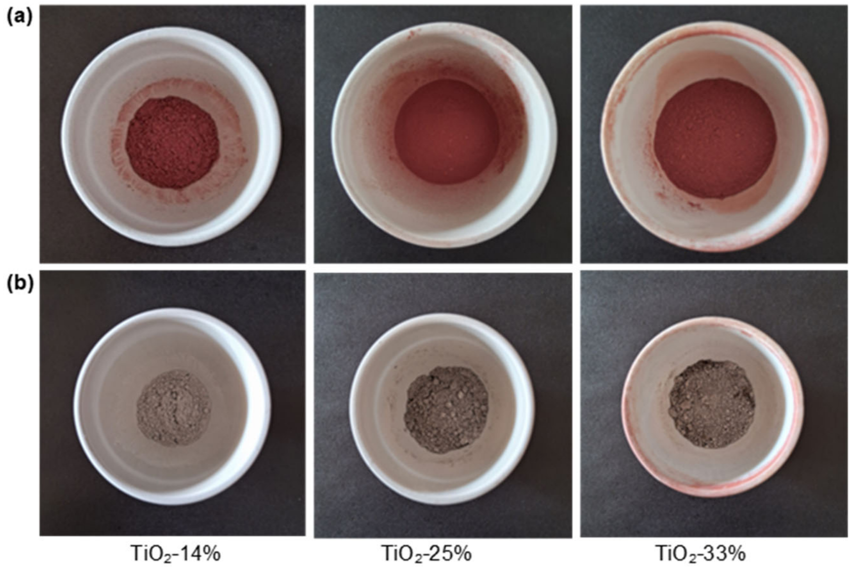

Fig 3. Green synthesis of TiO_2: (a) before and (b) after calcination

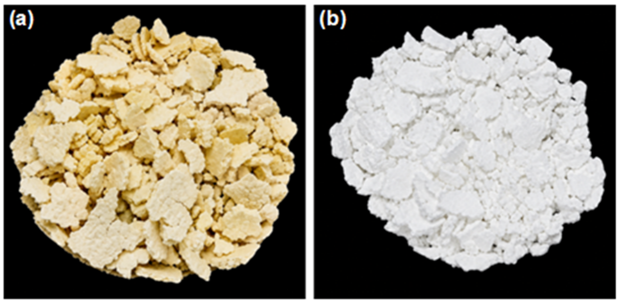

Fig 4. Conventional synthesis of TiO_2 (**a**) before and (**b**) after calcination

precursor into an ethanol solution and stirring for 1 h. After stirring, HNO_3 was added until the mixture reached pH 2. The addition of HNO_3 controlled the rates of hydrolysis and condensation, thereby preventing agglomeration and stabilizing the TiO_2 particles. The mixture was then stirred again for 1 h at 50 °C. The conventionally synthesized TiO_2 is shown in Fig. 4., appearing as a white powder and labeled as TiO_2-C. The yield obtained was 39.94%.

FTIR analysis of the sappan wood extract was carried out in the wavenumber range of 400–4000 cm^{-1}. The spectrum results shown in Fig. 5 indicate the presence of O–H stretching vibrations, with a broad peak observed at 3412 cm^{-1} the high-energy region. The peak in the FTIR spectrum of sappan wood extract is attributed to polyphenolic compounds. The hydroxyl groups in polyphenols play an important role in the reduction of metal ions and the formation of metal nanoparticles [16].

Other absorption peaks were observed at wavenumbers 2924 and 2855 cm^{-1}, corresponding to the C–H stretching vibrations of methyl ($-CH_3$) and methylene ($-CH_2$) groups. The absorption peak at 1709 cm^{-1} is assigned to the C=O stretching vibration of carbonyl groups. This peak indicates the presence of brazilein, which is the oxidation product of brazilin. The absorption peak at 1614 cm^{-1} corresponds to C=C stretching vibrations of the aromatic ring. The C=C stretching observed in the FTIR spectrum of sappan wood extract originates from brazilin, which is the major constituent of sappan wood. The absorption peak at 1034 cm^{-1} corresponds to C–O–C stretching vibrations of ether groups, while the peak at 854 cm^{-1} is attributed to the C–H bending vibration of substituted aromatic rings [17].

The absorption bands observed at 583 cm^{-1} (TiO_2-C), 594 cm^{-1} (TiO_2-14%), 559 cm^{-1} (TiO_2-25%), and 503 cm^{-1} (TiO_2-33%) in the respective TiO_2 spectra are attributed to Ti–O–Ti bonding [18]. The appearance of these absorption bands confirms the successful synthesis of TiO_2 using sappan wood (*B. sappan* L.) extract. Furthermore, the FTIR results (Fig. 5) indicate that phytochemicals present in the extract played a crucial role in reducing Ti^{4+} ions into TiO_2 particles. This is

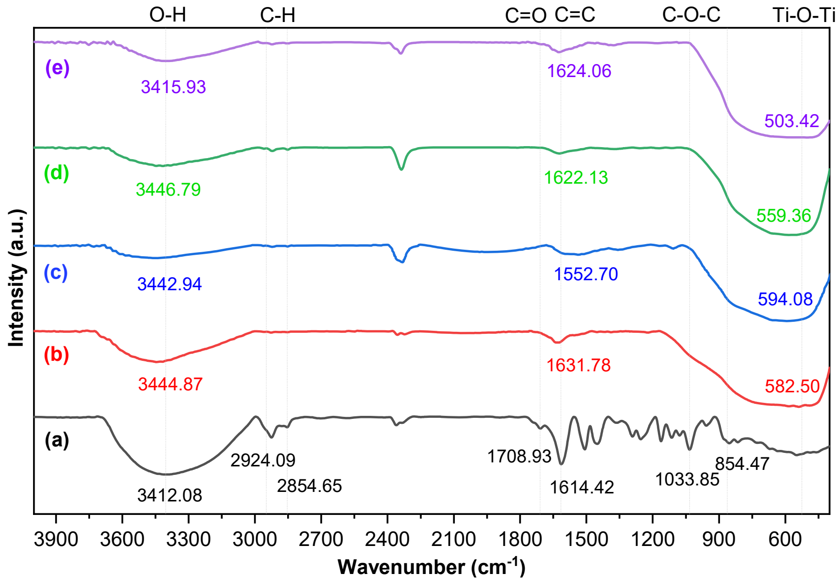

Fig 5. FTIR spectra (a) sappan wood extract, (b) TiO_2-C, (c) TiO_2-14% (d) TiO_2-25%, and (e) TiO_2-33%

evidenced by the decrease in the intensity of the functional groups from the extract in each TiO_2 spectrum [18].

XRD analysis in this study was carried out to determine the crystallite size and phase of TiO_2 synthesized by both green synthesis and conventional methods. The obtained diffractogram is shown in Fig. 6. The analysis was conducted within the 2θ range of 20°–80° and compared with the Joint Committee on Powder Diffraction Standards (JCPDS) File No. 01-078-2486. The X-ray diffraction patterns of TiO_2 synthesized through both green synthesis and conventional methods exhibited six major diffraction peaks with similar intensities.

The TiO_2 particles synthesized by the conventional method exhibited major diffraction peaks at 25.324°, 37.853°, 48.038°, 53.999°, 55.060°, and 62.711°, which correspond to the crystal planes (101), (004), (200), (105), (211), and (204), respectively. These results are consistent with the crystal planes obtained in TiO_2 synthesized via green synthesis using 5, 10, and 15 mL of sappan wood extract. The observed diffraction peaks agree with the standard anatase phase of TiO_2 (JCPDS File No. 01-078-2486). Based on the agreement of the crystal planes, it can be confirmed that TiO_2 synthesized through both green and conventional methods possesses an anatase phase.

Based on the diffractogram patterns shown in Fig. 6, additional information was obtained regarding the average crystallite size of each sample. The crystallite size was calculated using the Scherrer equation, and the results are presented in Table 2. The crystallite size is influenced by the full width at half maximum (FWHM) value, where a larger FWHM corresponds to a smaller crystallite size, and vice versa. This phenomenon occurs because smaller crystallites contain fewer lattice planes, resulting in broader diffraction peaks [19]. This phenomenon occurs because smaller crystallites contain fewer lattice planes, resulting in broader diffraction peaks. Furthermore, previous studies reported that increasing the annealing temperature promotes diffusion-driven crystal growth, in which the supplied thermal energy enhances atomic mobility, facilitates particle coalescence, and reduces grain boundary density, ultimately leading to the formation of larger, more ordered TiO_2 crystals. This phenomenon is evidenced by sharper XRD peaks, higher diffraction intensities, and lower FWHM values at elevated annealing temperatures, indicating improved crystallinity and grain growth. However, excessive crystal growth at very high temperatures may also induce particle agglomeration and surface deterioration, leading to a rougher film morphology and reduced structural quality [20]. Similar findings were also reported in TiO_2/ZnO nanocomposites synthesized via an electrochemical method, where enhanced crystallinity and well-ordered nanoparticle structures contributed to

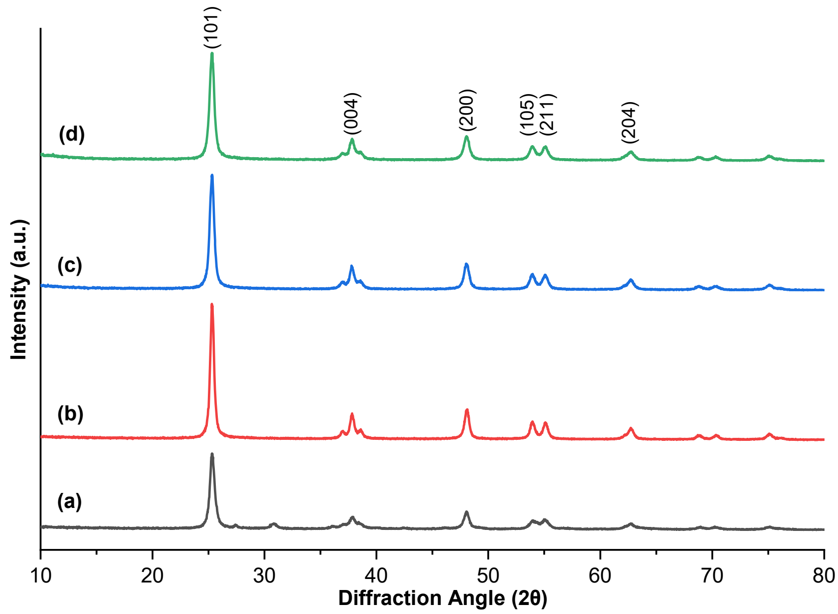

Fig 6. Diffractogram pattern (a) TiO_2-C (b) TiO_2-14% (c) TiO_2-25% (d) TiO_2-33%

Table 2. XRD data of TiO_2

Sample	Diffraction angle (2θ) (°)	θ (°)	θ (rad)	Cos θ	FWHM (°)	FWHM (rad)	β cos θ	D (nm)	D average (nm)
TiO_2-C	25.324	12.662	0.2209	0.9757	0.487	0.0085	0.0083	16.825	15.842
	37.853	18.927	0.3302	0.9460	0.692	0.0121	0.0114	12.213	
	48.038	24.019	0.4190	0.9135	0.531	0.0093	0.0085	16.482	
	53.999	27.000	0.4710	0.8911	0.460	0.0080	0.0072	19.503	
	55.060	27.530	0.4802	0.8869	0.509	0.0089	0.0079	17.710	
	62.711	31.356	0.5470	0.8541	0.760	0.0133	0.0113	12.316	
TiO_2-14%	25.352	12.676	0.2211	0.9757	0.396	0.0069	0.0067	20.693	19.747
	37.830	18.915	0.3300	0.9461	0.378	0.0066	0.0062	22.356	
	48.088	24.044	0.4194	0.9133	0.458	0.0080	0.0073	19.112	
	53.942	26.971	0.4705	0.8913	0.440	0.0077	0.0068	20.385	
	55.103	27.552	0.4806	0.8867	0.472	0.0082	0.0073	19.102	
	62.722	31.361	0.5471	0.8540	0.556	0.0097	0.0083	16.836	
TiO_2-25%	25.340	12.670	0.2210	0.9757	0.466	0.0081	0.0079	17.584	18.499
	37.814	18.907	0.3298	0.9461	0.348	0.0061	0.0057	24.282	
	48.059	24.030	0.4192	0.9134	0.542	0.0095	0.0086	16.149	
	53.903	26.952	0.4702	0.8915	0.454	0.0079	0.0071	19.753	
	55.050	27.525	0.4802	0.8869	0.494	0.0086	0.0076	18.247	
	62.721	31.361	0.5471	0.8541	0.625	0.0109	0.0093	14.978	
TiO_2-33%	25.321	12.661	0.2209	0.9757	0.480	0.0084	0.0082	17.070	16.583
	37.812	18.906	0.3298	0.9461	0.413	0.0072	0.0068	20.460	
	48.044	24.022	0.4191	0.9135	0.564	0.0098	0.0090	15.518	
	53.932	26.966	0.4704	0.8914	0.503	0.0088	0.0078	17.831	
	55.067	27.534	0.4803	0.8869	0.527	0.0092	0.0082	17.106	
	62.706	31.353	0.5469	0.8541	0.813	0.0142	0.0121	11.513	

improved optical properties and electron transfer efficiency, emphasizing the important role of crystallite growth in enhancing the functional performance of TiO_2-based nanomaterials [21].

The crystallite size calculation of TiO_2 synthesized using sappan wood extract showed that the average crystallite sizes of TiO_2-14%, TiO_2-25%, and TiO_2-33% were 19.7474, 18.4987, and 16.5831 nm, respectively. When compared with conventionally synthesized TiO_2 (TiO_2-C) with a crystallite size of 15.8416 nm, the crystallite sizes of the environmentally friendly synthesized samples show slight variations, although all samples remain in the nanoscale range. This difference may be influenced by the presence of phytochemicals, which influence nucleation and growth during synthesis. The reduction in crystallite size in the environmentally friendly-synthesized samples may be related to the capping effect of phytochemicals, which limits particle growth. These results indicate that the addition of sappan wood extract can serve as an alternative approach to producing TiO_2 particles with crystallite sizes in the nanometer range in an environmentally friendly manner.

UV-vis DRS analysis was conducted to determine the band gap energy of the synthesized TiO_2 (Fig. 7(a–d)). The measurements were carried out in the wavelength range of 200–800 nm. The obtained reflectance data (%R) were processed using the Kubelka Munk function to calculate the band gap energy. The resulting curves are presented in Fig. 8. The band gap energy (E_g) was determined from the relationship between the Kubelka Munk function (F(R)) and photon energy, where a straight line was extrapolated to intersect the X-axis, yielding the band gap energy values. Based on the curves shown in Fig. 7, the band gap values of TiO_2-C, TiO_2-14%, TiO_2-25%, and TiO_2-33% were 3.03, 2.53, 2.92, and 2.98 eV, respectively. These results indicate that the synthesized TiO_2 exhibits effective photocatalytic activity under UV irradiation [22]. Furthermore, the band gap values of TiO_2 samples synthesized with sappan wood extract were lower than those synthesized without the extract (conventional method). This finding suggests that the use of plant extract can reduce the TiO_2 band gap, which is attributed to the presence of defects or vacancies in the TiO_2 particles obtained through green synthesis [23]. Similar results were reported by De Luca et al. [9], where the band gap values of TiO_2 synthesized using plant extracts were lower compared to those prepared by the conventional route. In general, decreasing crystallite size can increase the bandgap energy due to quantum confinement effects. In this study, the relationship between crystallite size and bandgap is also influenced by factors beyond size effects. Several factors, including residual organic compounds from sappan wood extract, surface defects, and variations

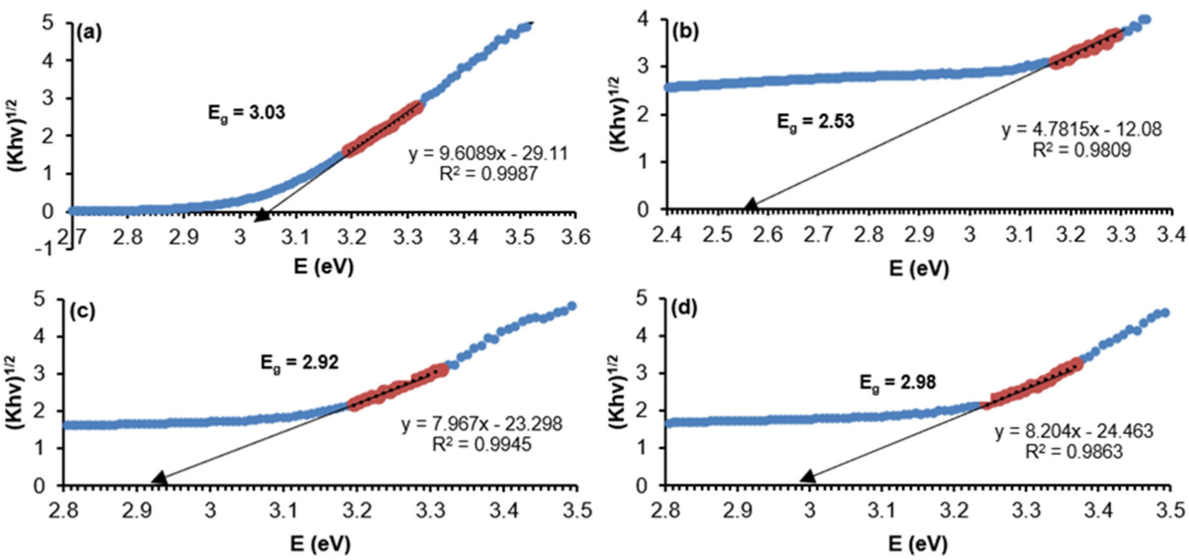

Fig 7. Plot curve of (a) TiO_2-C, (b) TiO_2-14%, (c) TiO_2-25%, (d) TiO_2-33%

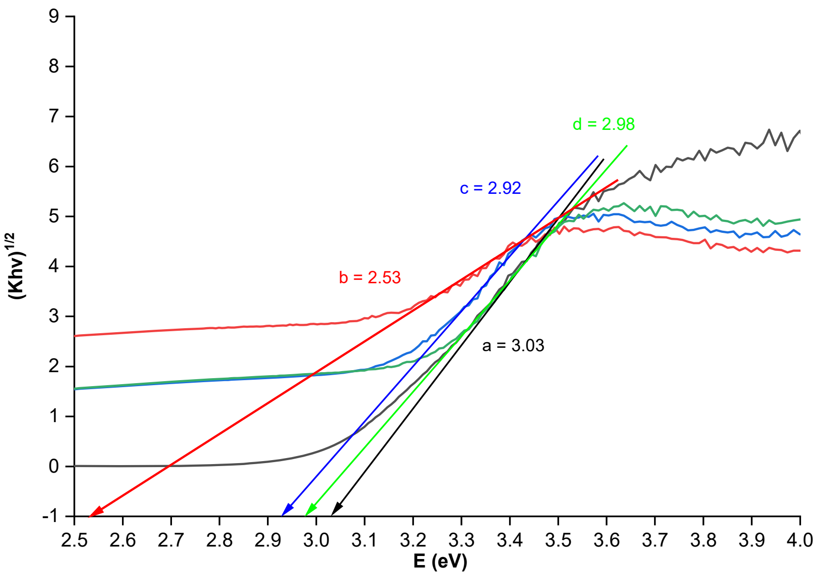

Fig 8. Kubelka Munk function plot curve of TiO_2-C, TiO_2-14%, TiO_2-25%, and TiO_2-33%

in crystallinity, can also influence the observed bandgap values. Phytochemicals acting as capping agents can affect the surface and electronic structure of TiO_2, leading to a narrowing of the bandgap or an irregular trend that deviates from the quantum confinement effect. The bandgap behavior observed in this study is likely due to the combined effects of crystallite size, surface chemistry, and structural properties.

The antibacterial activity test in this study was conducted to evaluate the antibacterial performance of TiO_2 against *E. coli* and *S. aureus*. The tested samples consisted of sappan wood extract, TiO_2-C suspension, TiO_2-14%, TiO_2-25%, and TiO_2-33%. Each sample was prepared at a concentration of 450 μg/mL in DMSO. The antibacterial assay employed two types of controls: a positive control using streptomycin and a negative control using DMSO.

The use of a positive control served as a reference to compare the antibacterial performance of the synthesized TiO_2 with a commonly used antibiotic. The negative control was employed to determine the effect of the solvent on bacterial growth, since DMSO was used as the solvent in the preparation of the TiO_2 suspensions [24]. The antibacterial activity test in this study was carried out under both visible light and UV irradiation to compare the antibacterial activity results under the two irradiation conditions. The antibacterial activity was quantitatively evaluated by measuring the diameter of the inhibition zones formed.

The antibacterial activity test results of sappan wood extract and TiO_2 variations under visible light are presented in Fig. 9. Based on Fig. 9, the extract exhibited antibacterial activity against both *E. coli* and *S. aureus*, as indicated by the formation of inhibition zones around the discs treated with the extract. The observed antibacterial activity of the extract is attributed to the presence of bioactive compounds such as flavonoids, tannins, and other phytochemicals contained in the sappan wood [13].

The synthesized TiO_2 samples, both without extract (TiO_2-C) and with extract (TiO_2-14%, TiO_2-25%, and TiO_2-33%), did not exhibit antibacterial activity.

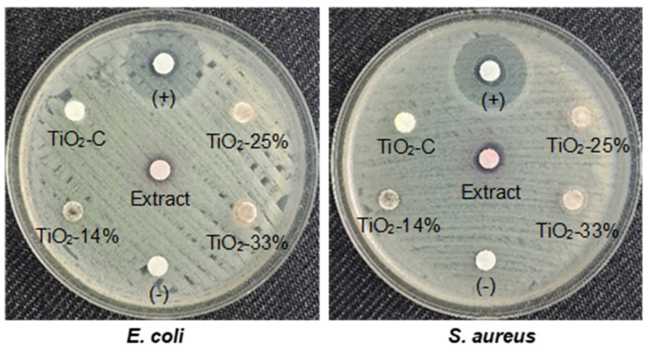

Fig 9. Antibacterial activity test result under visible light irradiation

This was indicated by the absence of inhibition zones around the discs treated with the test samples. The band gap energy values of the four synthesized TiO_2 samples ranged from 2.53 to 3.03 eV, within which the photocatalytic properties of TiO_2 are generally expected to perform effectively under visible light irradiation. However, the observed results differed, which may be due to the light source providing insufficient or suboptimal photon energy to excite electrons from the valence band to the conduction band of TiO_2. As a result, the formation of electron-hole pairs and reactive oxygen species (ROS), which subsequently contribute to photocatalytic and antibacterial activities, is limited.

The antibacterial activity test results of sappan wood extract and TiO_2 variations under UV light are shown in Fig. 10. Similar results were obtained for sappan wood extract, where inhibition zones were observed around the discs against both *E. coli* and *S. aureus*. This indicates that, under both visible and UV light irradiation, sappan wood extract exhibits antibacterial activity. In contrast, the antibacterial activity test results for the TiO_2 samples under UV irradiation showed different outcomes compared to those obtained under visible light irradiation.

The formation of inhibition zones in the TiO_2-14%, TiO_2-25%, and TiO_2-33% samples indicates that these samples exhibit antibacterial activity. The presence of inhibition zones in these samples is attributed to the photocatalytic properties of TiO_2, which perform more effectively under UV irradiation. The photocatalytic activity of TiO_2 can generate ROS such as $\bullet O_2^-$, $\bullet OH$, and H_2O_2. These radicals are capable of reacting with organic compounds in the bacterial cell membrane, such as the peptidoglycan layer, leading to bacterial cell lysis [24]. The schematic illustration of the photocatalytic mechanism of TiO_2 under light irradiation and ROS responsible for antibacterial activity shown in Fig. 11.

Based on Table 3, the inhibition zone diameter for *S. aureus* was larger compared to *E. coli*. The difference in antibacterial effectiveness of TiO_2 against *E. coli* and *S. aureus* is attributed to the structural differences in their cell walls. *E. coli* is classified as a Gram-negative bacterium, whose cell wall consists of a thin peptidoglycan layer but is reinforced by a thick and rigid outer membrane composed of lipopolysaccharides. This makes the cell wall of Gram-negative bacteria more complex compared to Gram-positive bacteria, such as *S. aureus*, which possesses a thick cell wall composed mainly of peptidoglycan [6]. In addition, previous studies have demonstrated that biofunctionalized TiO_2 nanoparticles exhibit excellent stability and biocompatibility, enabling

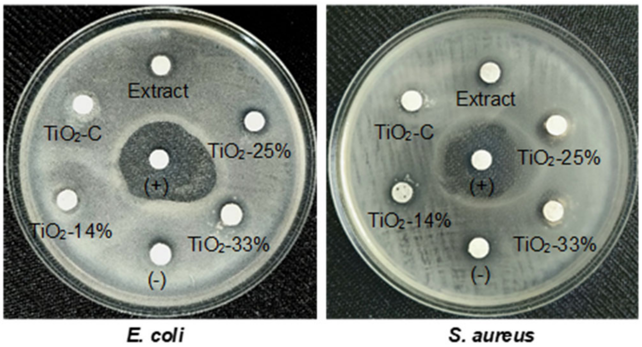

Fig 10. Antibacterial activity test result under UV light irradiation

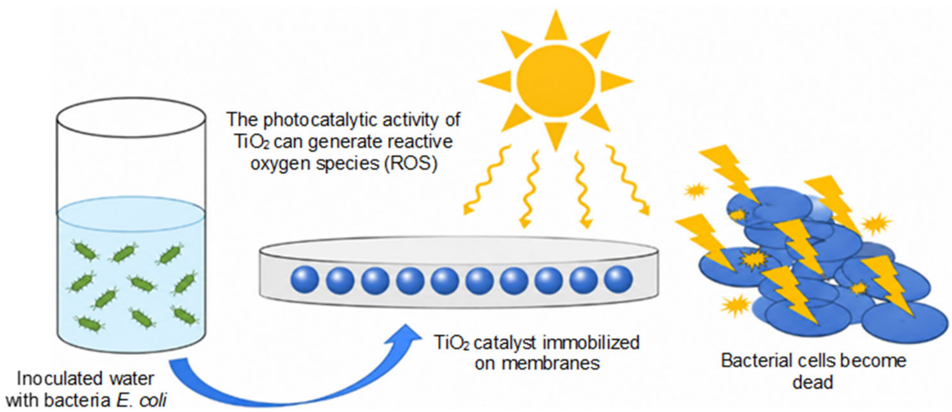

Fig 11. Schematic illustration of the photocatalytic mechanism of TiO_2 for antibacterial activity

Table 3. Inhibition zone diameter against *E. coli* and *S. aureus* under visible and UV light irradiation

Sample	Inhibition zone diameter (mm)			
	Visible light		UV light	
	E. coli	*S. aureus*	*E. coli*	*S. aureus*
Extract	1.2	3.9	2.7	2.1
TiO_2-C	-	-	-	-
TiO_2-14%	-	-	2.8	2.2
TiO_2-25%	-	-	3.0	5.9
TiO_2-33%	-	-	5.1	6.2
Control (+)	16.2	15.7	21.2	16.6
Control (−)	-	-	-	-

more effective interactions with biological systems. TiO_2-based nanomaterials have also been reported to exhibit enhanced bioactivity and controlled release properties, indicating strong potential not only as antibacterial agents but also as efficient nanocarriers for biomedical applications, including targeted drug delivery and cancer therapy [25].

CONCLUSION

This study demonstrates that phytochemical constituents in plant extracts not only facilitate nanoparticle formation but also modify the energy band gap, thereby enhancing photocatalytic activity under UV irradiation. In contrast to conventionally synthesized TiO_2, the green-synthesized TiO_2 exhibited significant antibacterial activity against *E. coli* and *S. aureus*, which was attributed to the enhanced ROS formation that disrupt bacterial cell integrity. These findings highlight the potential of green-engineered TiO_2 nanomaterials as eco-friendly photocatalytic antibacterial agents for environmental and biomedical applications.

ACKNOWLEDGMENTS

This work was supported by grants from the Mathematics and Natural Sciences Faculty, Universitas Tanjungpura Pontianak, under DIPA UNTAN Grant No.SP DIPA-023.17.2.677517/2024. The authors express great gratitude for that support.

CONFLICT OF INTEREST

All authors have no conflicts of interest related to this manuscript.

AUTHOR CONTRIBUTIONS

Risya Sasri designed the methodology, wrote and revised the manuscript, Vika conducted the experiments and wrote the draft, Adhitiyawarman checked the manuscript for accuracy, and Winda Rahmalia checked the data for accuracy and revised the manuscript. All authors approved the final version of this manuscript.

REFERENCES

[1] Eddy, D.R., Permana, M.D., Sakti, L.K., Sheha, G.A.N., Solihudin, S., Hidayat, S., Takei, T., Kumada, N., and Rahayu, I., 2023, Heterophase polymorph of TiO_2 (anatase, rutile, brookite, TiO_2 (B)) for efficient photocatalyst: Fabrication and activity, *Nanomaterials*, 13 (4), 704.

[2] Verma, V., Al-Dossari, M., Singh, J., Rawat, M., Kordy, M.G.M., and Shaban, M., 2022, A review on green synthesis of TiO_2 NPs: Photocatalysis and antimicrobial applications, *Polymers*, 14 (7), 1444.

[3] Kaur, H., Kaur, S., Kumar, S., Singh, J., and Rawat, M., 2020, Eco-friendly approach: Synthesis of novel green TiO_2 nanoparticles for degradation of Reactive Green 19 dye and replacement of chemical synthesized TiO_2, *J. Cluster Sci.*, 32 (5), 1191–1204.

[4] Insuan, W., Sillawatthumrong, N., Chahomchuen, T., Khamchun, S., Chueahongthong, F., and Insuan, O., 2024, Brazilin content and potential biological properties of *Caesalpinia sappan* L. heartwood extracts from different extraction methods, *Discover Appl. Sci.*, 6 (10), 509.

[5] Younis, A.B., Milosavljevic, V., Fialova, T., Smerkova, K., Michalkova, H., Svec, P., Antal, P., Kopel, P., Adam, V., Zurek, L., and Dolezelikova, K., 2023, Synthesis and characterization of TiO_2 nanoparticles combined with geraniol and their synergistic antibacterial activity, *BMC Microbiol.*, 23 (1), 207.

[6] Tavares, T.D., Antunes, J.C., Padrão, J., Ribeiro, A.I., Zille, A., Amorim, M.T.P., Ferreira, F., and Felgueiras, H.P., 2020, Activity of specialized biomolecules against Gram-positive and Gram-negative bacteria, *Antibiotics*, 9 (6), 314.

[7] Dubale, S., Kebebe, D., Zeynudin, A., Abdissa, N.,

and Suleman, S., 2023, Phytochemical screening and antimicrobial activity evaluation of selected medicinal plants in Ethiopia, *J. Exp. Pharmacol.*, 15 (1), 51–62.
[8] Mathew, S.S., Sunny, N.E., and Shanmugam, V., 2021, Green synthesis of anatase titanium dioxide nanoparticles using *Cuminum cyminum* seed extract; Effect on mung bean (*Vigna radiata*) seed germination, *Inorg. Chem. Commun.*, 126, 108485.
[9] De Luca, A., De Benedetto, A., De Matteis, V., Cascione, M., Di Corato, R., Ingrosso, C., Corrado, M., and Rinaldi, R., 2024, Eco-friendly TiO_2 nanoparticles: Harnessing aloe vera for superior photocatalytic degradation of methylene blue, *Catalysts*, 14 (11), 820.
[10] Subhapriya, S., and Gomathipriya, P., 2018, Green synthesis of titanium dioxide (TiO_2) nanoparticles by *Trigonella foenum-graecum* extract and its antimicrobial properties, *Microb. Pathog.*, 116, 215–220.
[11] Geow, C.H., Tan, M.C., Yeap, S.P., and Chin, N.L., 2021, A review on extraction techniques and its future applications in industry, *Eur. J. Lipid Sci. Technol.*, 123 (4), 2000302.
[12] Rajput, M.S., Nirmal, N.P., Nirmal, S.J., and Santivarangkna, C., 2022, Bio-actives from *Caesalpinia sappan L.*: Recent advancements in phytochemistry and pharmacology, *S. Afr. J. Bot.*, 151, 60–74.
[13] Vij, T., Anil, P.P., Shams, R., Dash, K.K., Kalsi, R., Pandey, V.K., Harsanyi, E., Kovács, B., and Shaikh, A.M., 2023, A comprehensive review on bioactive compounds found in *Caesalpinia sappan*, *Molecules*, 28 (17), 6247.
[14] Langa, C., and Hintsho-Mbita, N.C., 2023, Plant and bacteria mediated synthesis of TiO_2 NPs for dye degradation in water. A review, *Chem. Phys. Impact*, 7, 100293.
[15] Aslam, M., Abdullah, A.Z., and Rafatullah, M., 2021, Recent development in the green synthesis of titanium dioxide nanoparticles using plant-based biomolecules for environmental and antimicrobial applications, *J. Ind. Eng. Chem.*, 98, 1–16.
[16] Nasrollahzadeh, M., Sajadi, S.M., Rostami-Vartooni, A., and Hussin, S.M., 2016, Green synthesis of CuO nanoparticles using aqueous extract of *Thymus vulgaris* L. leaves and their catalytic performance for *N*-arylation of indoles and amines, *J. Colloid Interface Sci.*, 466, 113–119.
[17] Ngamwonglumlert, L., Devahastin, S., Chiewchan, N., and Raghavan, G.S.V., 2020, Color and molecular structure alterations of brazilein extracted from *Caesalpinia sappan* L. under different pH and heating conditions, *Sci. Rep.*, 10 (1), 12386.
[18] Ahmad, W., Jaiswal, K.K., and Soni, S., 2020, Green synthesis of titanium dioxide (TiO_2) nanoparticles by using *Mentha arvensis* leaves extract and its antimicrobial properties, *Inorg. Nano-Met. Chem.*, 50 (10), 1032–1038.
[19] Bunaciu, A.A., Udriştioiu, E.G., and Aboul-Enein, H.Y., 2015, X-ray diffraction: Instrumentation and applications, *Crit. Rev. Anal. Chem.*, 45 (4), 289–299.
[20] Safiay, N.M., Abdul Rani, R., Ahmed Azhar, N.E., Khusaimi, Z., Hamzah, F., and Rusop, M., 2021, Influence of different annealing temperatures on the structural and optical properties of TiO_2 nanoparticles synthesized via sol-gel method: Potential application as UV sensor, *Indones. J. Chem.*, 21 (2), 279–285.
[21] Alduhaidahawi, A.M.J., and Ahmed, A.A., 2024, Synthesis of TiO_2/ZnO nanocomposites by the electrochemical method and their application in dye-sensitized solar cells (DSSCs), *Indones. J. Chem.*, 24 (1), 228–237.
[22] Kassalia, M.E., Chorianopoulos, N., Nychas, G.J., and Pavlatou, E.A., 2023, Investigation of the photoinduced antimicrobial properties of N-doped TiO_2 nanoparticles under visible-light irradiation on *Salmonella typhimurium* biofilm, *Appl. Sci.*, 13 (7), 4498.
[23] Pathinti, R.S., Gollapelli, B., Jakka, S.K., and Vallamkondu, J., 2021, Green synthesized TiO_2 nanoparticles dispersed cholesteric liquid crystal systems for enhanced optical and dielectric properties, *J. Mol. Liq.*, 336, 116877.
[24] Maryani, E., Nurjanah, N.S., Hadisantoso, E.P., and Wijayanti, R.B., 2020, The effect of TiO_2 additives on the antibacterial properties (*Escherichia coli* and

Staphylococcus aureus) of glaze on ceramic tiles, *IOP Conf. Ser.: Mater. Sci. Eng.*, 980 (1), 012011.
[25] Rahujo, S., Talpur, F.N., Laghari, A.Q., Mert, O., Afridi, H.I., Ali, Z., Razzaque, N., Chandio, I., Zaman, N., and Abro, M., 2026, Biofunctionalized titanium dioxide nanoparticles with bovine serum albumin for targeted cytotoxicity in MCF-7 breast cancer cells, *Indones. J. Chem.*, 26 (2), 462–471.